Characterization of non-premixed Hydrogen-oxygen flame heights by chemical luminescence imaging and LDV techniques

J-L. Beduneau, D. Honore and M. Boukhalfa

LAME-CORIA UMR 6614 CNRS
INSA- Avenue de l'Université-BP8
76801 Saint-Etienne-du-Rouvray Cedex
France

E-mail: boukhalfa@coria.fr

Introduction

The turbulent non-premixed turbulent jet flame length is an important indicator of mixing process, since flame length is found to be proportional to the axial distance required to dilute the fuel mixture fraction to its stoechiometric value. The principal problem is to define the flame height. In fact, the visible length of a non-premixed jet flame is an easy way to determine this characteristic scale, but this location can be fixed by several manner. The maximal height where gas burnt at a sufficient frequency [2]. The maximal height where the flame radiate in the visible at a sufficient frequency [3]. The maximal height reach by the visible flame flapping [4]. Each definition can be considered correct but without any doubt they can't represent the same flame length.
In this study, two different and complementary techniques have been used to evaluate this characteristic scale. The LDV technique was adapted to measure the flame length from the axial velocity evolution and from the location of the axial velocity fluctuation increasing (Fig 4), whereas the OH chimiluminescence is employed to determine the flame length from the maximum OH axial intensity emission (Fig 5).
Experimental results are compared with thus obtained from Driscoll & al [1] formulation (equ. 1) with scaling arguments previously presented by Hawthorne & al [4], Becker and Liang [5], schlichting [6] and Dahm & Dibble [7].

$$\frac{L_f}{d_f} = c_1 \left(\frac{\rho_{O_2} U_{O_2}}{\rho_{H_2} U_{H_2}} \right)^{\frac{1}{2}} \left(\frac{U_{O_2}}{U_{H_2} - U_{O_2}} \right)^{\frac{1-n}{2n}} f_s^{\frac{-1}{2n}} \qquad \textbf{equ. 1.}$$

Where f_s is the stoichiometric mixture fraction, which is 0.125 for hydrogen-oxygen reactions. The exponent n for this experimental configuration is treated as unknown, and C_1 is a constant.

Experimental configuration

Hydrogen-oxygen flames are stabilized on an axisymmetric coaxial injector (Fig. 1), where oxygen is injected in the internal tube, with a mean velocity close to 5 m/s and hydrogen in the outside one, with a mean exit velocity close to 60 m/s. The combustion occurs at atmospheric pressure in an open square transparency combustion chamber of 60*60 mm². In this work, two geometrical configurations of coaxial injectors were studied. The main characteristics are presented in Table 1. In order to simulate the conditions in a rocket gas generator, injectors operate with an important excess of hydrogen (Table 2). In such experimental conditions, the non-premixed hydrogen-oxygen flame is stabilized at the exit of the injector without pilot flame, and the excess of hydrogen is burned with the ambient air at the exit of the open combustion chamber.

The dynamic structure of each flame is investigated by performing Laser Doppler Velocimetry (LDV) The LDV system is a two color, dual beam TSI system. Axial and radial velocity components are measured using respectively the green and the blue lines, from a 6W Argon-Ion laser. Directional ambiguity is eliminated by frequency shifting (40 Mhz on each beam pair). The LDV signal is processed by an IFA 750 Digital Burst Correlator. Both hydrogen and oxygen jets were seeded with Zirconium Oxide (ZrO2, diameter ≈ 2 μm) introduced in the flow by two rotate brush seeders. The LDV probe volume can be assumed to a cylindrical volume with 1.2 mm length and 90 μm diameter.
The axial position of the oxygen potential core end (increase of fluctuation) has been used as a definition of the flame length (L_{flame}) for each flame conditions [Fig. 4]
In the present experiment, instantaneous flame front imaging has been performed by chemiluminescence imaging of excited OH radicals. This optical technique is a relatively simple method to obtain information on instantaneous and mean structures of turbulent flames without the need of a complex experimental bench [8].
The experimental set-up consists mainly of an ICCD camera (Princeton Instruments IMAX) equipped with a UV lens (Nikkor 105 mm - f/4.5) and a UG11 filter. The latter enables us to select a UV spectral range transmitted to the camera, corresponding to the main rovibronic transitions of the ($A^2\Sigma^+ \rightarrow X^2\Pi_i$) system of OH radicals. The ICCD camera is gated with an intensification time of 10 μs. This gated time is sufficiently low to consider the flow as "frozen", i.e. to obtain instantaneous flame front images.
For each condition, statistical study of 1000 instantaneous images has been conducted in order to construct the mean and RMS flame front images. Because of the integration of the OH chemiluminescence signal along the light of sight, the obtained images can not be directly related to the local spontaneous emission of the flame, and have to be analyzed cautiously.
However, whatever the flame conditions, one always observes an increase of the mean axial signal of OH chemiluminescence up to a maximum, from where the signal decreases. As OH radicals chemiluminescence is only present in the flame front and corresponds to the maximum of the heat release density, this region can be related to the top of the flame. Thus, the axial position of the maximum of mean OH spontaneous emission has been used as a definition of the flame length (L_{flame}) for each flame conditions [Fig. 5].
Moreover, thanks to the axisymetry of the burner, post-processing of the mean integrated image by Abel's inversion algorithm allows us to reconstruct the image of the mean radial location of the flame front . This method has been validated in the present experiment by comparison with OH PLIF measurements previously obtained for one flame conditions [9].

Experimental results

Figures 2 and 3 present respectively an example of axial velocity and OH chemiluminescence fields obtained for flame LF3 and LF4, used to determine the flame length. Velocity measurements are very complicate as the flame produces a high temperature level (3000K) and velocity gradients are very important [10].
Calculation given by the Driscoll & al formulation [1] contain two unknown parameters, C_1 and n. these two empirical values determined experimentally in subsonic and supersonic flames as a constant values are in fact depending on dynamic conditions. This important result is shown on Figures 7 and 8 which present an example of C_1 and n determination by fitting the equ. 1 with introducing LDV results obtained. We can note that C_1 seems to be a linear function of oxygen mass flux. This evolution is not depending on the injector configuration geometry and the slope determining the linear tendancy is constant for the two injectors studied. the same behavior is observed for n values. Then, by introducing these evolutions a formulation derived from the Driscoll & al [1] one is obtained :

$$\frac{L_f}{d_f} = 0.35(U_{O_2}+1)\left(15.83\frac{U_{O_2}}{U_{H_2}}\right)^{\frac{1}{2}}\left(\frac{U_{O_2}}{U_{H_2}-U_{O_2}}\right)^{\frac{1-(xU_{O_2}+y)}{2(xU_{O_2}+y)}} f_s^{\frac{-1}{2(xU_{O_2}+y)}} \qquad \textbf{equ. 2.}$$

With for injector 1: x=-0.065 and y=1.51
And for injector 2: x=-0.23 and y=2.3

The measured and calculated flame lengths are summarized in Table 2, globally a good agreement is observed. A quasi-constant difference between these results is observed, it is certainly due to the flame length definition which is different for each techniques. Difference between theoretical and experimental results are lower than 10 %, and it is probably due partly to flow rate measurement uncertainties.

Conclusion

The main objective of this investigation was to determine the non-premixed hydrogen-oxygen flame length with a high accuracy. In this way, the Driscoll & al [1] formulation has been adapted to the rocket engine injector configuration.
A very good agreement has been obtained for each injectors and for several conditions between two different experimental flame height determination and the formulation used.
In order to valid the determination of the n and C_1 coefficients a near set of experiments for a larger range of flow rate scale is needed.

References

[1] James F. Driscoll, Hwanil HuH, Youngbin Yoon, and Jeffrey Donbar. 1996, Combustion and Flame, vol. 107, p.176
[2] Becker H & Liang D. 1978, Combustion and Flame, vol. 32 p. 115.
[3] Driscoll J, Chen R & Yoon Y. 1992, Combustion and Flame, 88.
[4] Hawthorne W., Weddel D. & Hottel H. 1948, 3rd Symposium (International) on combustion, The Combustion Institute, Pittsburg, p.266.
[5] Becker, H., and Liang, D. 1978, Combustion and Flame, vol. 32, p. 115.
[6] Schlichting, H., 1968, *Boundary Layer Theory*, Mc Graw Hill, New York.
[7] Dahm, W. J. A., and Dibble, R. W., Twenty-Second Symposium (International) on Combustion, The Combustion Institute, Pittsburgh, p. 801.
[8] D. Honoré, D. Jaffré, M. Perrin, K. Mokaddem, J.C. Rolon, A. Susset, 1998, International Gas Research Conference 98, San Diego.
[9] J-C. Sacadura, 1997, Thèse de Doctorat de l'Université de Rouen.
[10] J.L. Beduneau, A. Boukhalfa and G. Cabot, 2000, 10th International Symposium on Applications of Laser Techniques to Fluid Mechanics, Lisbon.

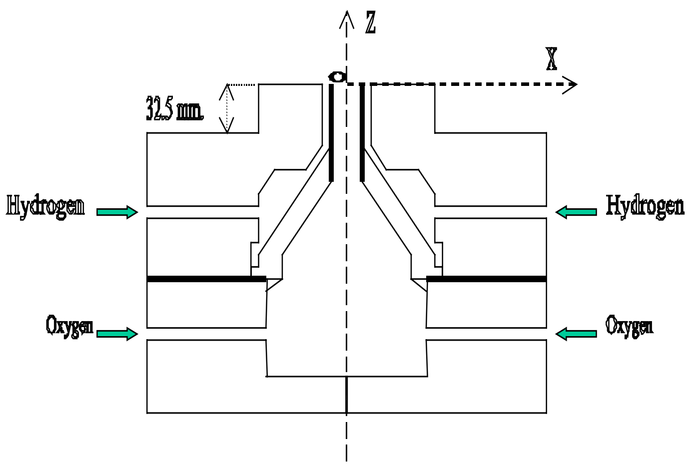

Fig. 1: *Coaxial injector*

	Diameter internal tube	Diameter external tube	Lip thickness
Injector 1	5.1 mm	9.1 mm	0.8 mm
Injector 2	6.6 mm	11.7 mm	0.8 mm

Table 1: *Geometrical characteristics of injectors*

	Hydrogen flow rate (g/s)	Hydrogen exit velocity (m/s)	Oxygen flow rate (g/s)	Oxygen exit velocity (m/s)	Flow rate ratio	length OH mm	Length LDV mm	Length (mm)
LF1	0.22	88	0.153	5.6	0.7	30.0	30.6	33.9
LF2	0.17	68	0.153	5.6	0.9	33.5	33.5	37.8
LF3	0.14	56	0.153	5.6	1.1	35.8	36.3	41.2
LF4	0.11	44	0.153	5.6	1.3	38.7	37.6	45.7
LF5	0.11	44	0.077	2.8	0.7	16.6	18.6	20.5
LF6	0.085	34	0.077	2.8	0.9	19.9	20.1	22.5
LF7	0.38	82	0.256	5.6	0.7	43.3	44.5	45.0
LF8	0.29	63	0.256	5.6	0.9	49.5	50.3	51.2
LF9	0.24	52	0.256	5.6	1.1	55.6	53.2	56.3
LF10	0.19	41	0.256	5.6	1.3	62	56.7	63.3
LF11	0.19	41	0.129	2.8	0.7	29.1	29.1	28.7
LF12	0.15	34	0.129	2.8	0.9	30.8	30.5	30.5

Table 2: *Flow fields conditions*

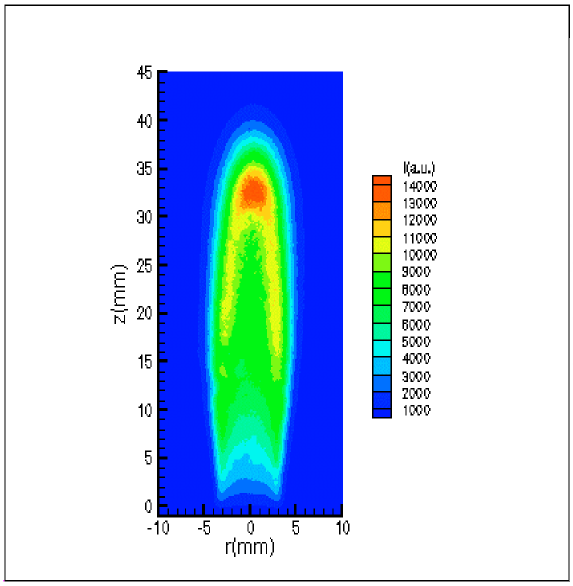

Fig 2: *Mean intensity of OH chemiluminescence, LF4*

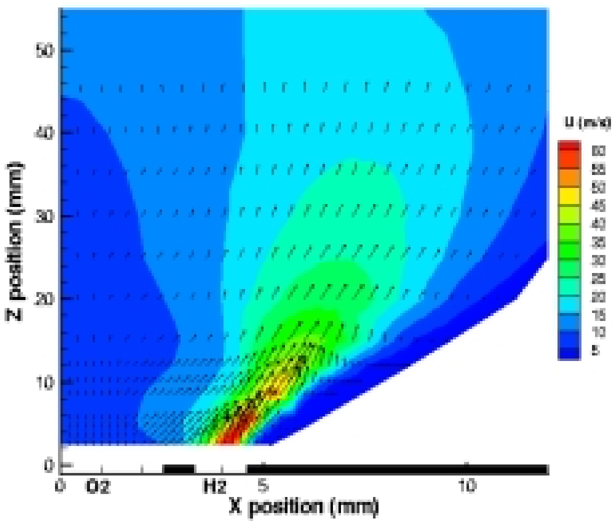

Fig 3: *Mean axial velocity field and velocity vectors, LF3*

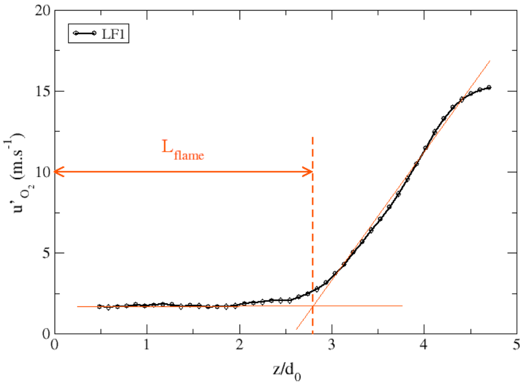

Fig 4: Mean **a**xial velocity evolution, LF1

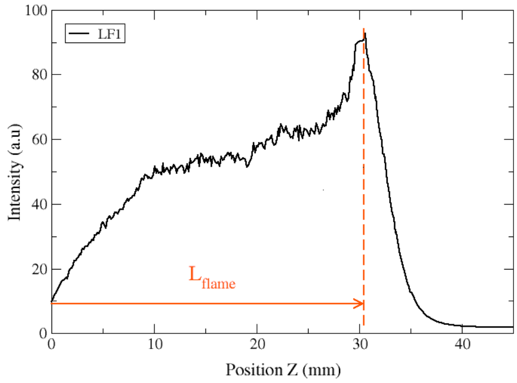

Fig 5: *Mean axial OH chemiluminescence evolution*

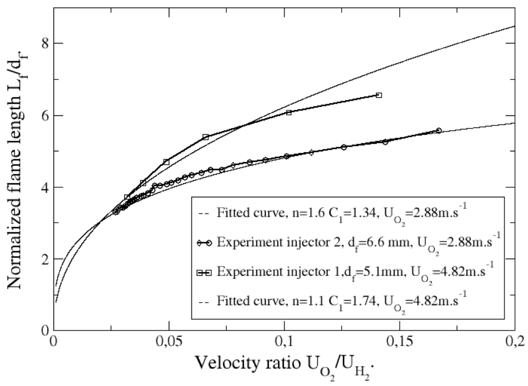

Fig 6: *Experimental and theoretical fitting*

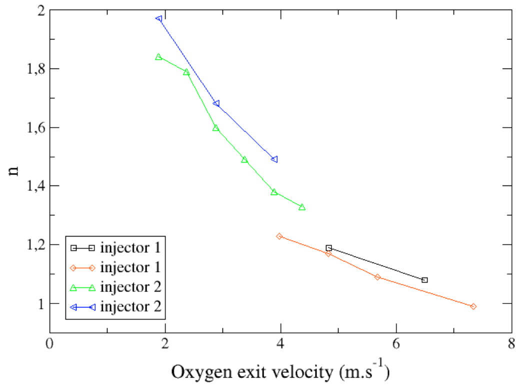

Fig 7: *n factor determination*

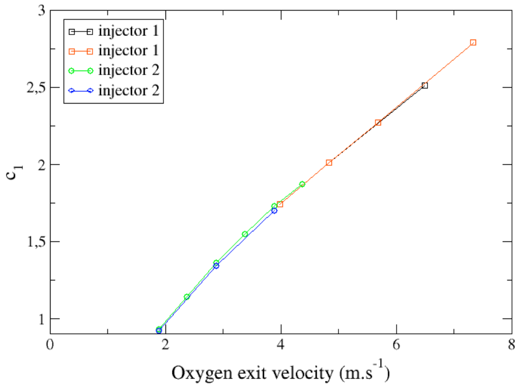

Fig 8: C_1 *factor determination*